EXOSKELETONS

Exoskeletons need to react faster than physiological responses to improve standing balance

Owen N. Beck[1,2]*†, Max K. Shepherd[3,4]†, Rish Rastogi[2], Giovanni Martino[2], Lena H. Ting[2,5]‡, Gregory S. Sawicki[6,7]‡

Maintaining balance throughout daily activities is challenging because of the unstable nature of the human body. For instance, a person's delayed reaction times limit their ability to restore balance after disturbances. Wearable exoskeletons have the potential to enhance user balance after a disturbance by reacting faster than physiologically possible. However, "artificially fast" balance-correcting exoskeleton torque may interfere with the user's ensuing physiological responses, consequently hindering the overall reactive balance response. Here, we show that exoskeletons need to react faster than physiological responses to improve standing balance after postural perturbations. Delivering ankle exoskeleton torque before the onset of physiological reactive joint moments improved standing balance by 9%, whereas delaying torque onset to coincide with that of physiological reactive ankle moments did not. In addition, artificially fast exoskeleton torque disrupted the ankle mechanics that generate initial local sensory feedback, but the initial reactive soleus muscle activity was only reduced by 18% versus baseline. More variance of the initial reactive soleus muscle activity was accounted for using delayed and scaled whole-body mechanics [specifically center of mass (CoM) velocity] versus local ankle—or soleus fascicle—mechanics, supporting the notion that reactive muscle activity is commanded to achieve task-level goals, such as maintaining balance. Together, to elicit symbiotic human-exoskeleton balance control, device torque may need to be informed by mechanical estimates of global sensory feedback, such as CoM kinematics, that precede physiological responses.

INTRODUCTION

The erect bipedal posture of the human body makes it inherently difficult to maintain balance during everyday tasks. To simply maintain standing balance, a human's relatively high center of mass (CoM) with respect to a small base of support and intrinsically compliant legs necessitates constant active muscle force production (1–3). After a disturbance, physiological processes take about 130 ms before ankles begin producing reactive balance-correcting joint moments (4, 5). This long latency limits a person's ability to regain postural equilibrium (6, 7) and is primarily due to the time required for neural conduction and processing (8). To compensate for these morphological limitations, researchers have begun developing wearable exoskeletons to improve human balance during everyday life (9–14).

Exoskeletons may be able to improve human balance by reacting to postural disturbances faster than physiologically possible. That is, electromechanical machines, such as exoskeletons, can detect mechanical changes and provide torque to limb joints faster than humans can evoke reactive joint moments (11, 15, 16). By preceding human physiological responses, "artificially fast" torque production can theoretically provide balance-correcting assistance by rapidly moving the user's limbs and shifting their center of pressure to help decelerate the perturbed CoM.

Conversely, the effectiveness of artificially fast exoskeleton torque in restoring user balance may be diminished because of the disruption of underlying physiology. Although simple inverted pendulum dynamics suggest that artificially fast exoskeleton torque production can improve balance (3, 5), artificially fast exoskeleton torque may inhibit the user's initial balance-correcting responses by disrupting sensory input (5, 12, 17), yielding suboptimal human-exoskeleton balance control. After a postural disturbance, the initial reactive muscle activity that produces measurable joint moments is well explained by delayed and scaled CoM kinematics (17–19) and is thought to be driven by proprioceptive sensory information from throughout the body (17). For example, regardless of how perturbations alter ankle-joint or plantar flexor muscle mechanics (18, 20, 21), there remains notable initial reactive plantar flexor muscle activity to help decelerate the perturbed CoM (18, 20, 21). Thus, if artificially fast exoskeleton torque quickly decelerates the perturbed CoM and/or reduces proprioceptor firing rates throughout the body, the ensuing initial reactive agonist muscle activity may also decrease. However, experimental data from balance-improving exoskeletons yield conflicting evidence regarding whether device torque decreases or increases initial reactive agonist muscle activity (11, 12). Furthermore, exoskeleton studies suggest that device torque increases antagonist (dorsiflexor) muscle activity versus baseline, indicating that users resist artificially fast device movements (22–24).

Delaying exoskeleton torque to complement the user's unaltered physiological response may elicit ideal human-exoskeleton balance control. Such "physiologically delayed" torque could be implemented using myoelectric or electroencephalographic control (25–27).

[1]Department of Kinesiology and Health Education, University of Texas at Austin, Austin, TX, USA. [2]Wallace H. Coulter Department of Biomedical Engineering, Emory University and Georgia Institute of Technology, Atlanta, GA, USA. [3]Department of Physical Therapy and Rehabilitation Science, Northeastern University, Boston, MA, USA. [4]Department of Mechanical and Industrial Engineering, Northeastern University, Boston, MA, USA. [5]Department of Rehabilitation Medicine, Division of Physical Therapy, Emory University, Atlanta, GA, USA. [6]George W. Woodruff School of Mechanical Engineering, Georgia Institute of Technology, Atlanta, GA, USA. [7]School of Biological Sciences, Georgia Institute of Technology, Atlanta, GA, USA.
*Corresponding author. Email: owen.beck@austin.utexas.edu
†These authors contributed equally to this work.
‡These authors contributed equally to this work.

Functionally, delaying exoskeleton torque onset would effectively scale the user's initial reactive joint moments after a perturbation. In turn, such supplemented joint moments may better keep the user within their limits of stability (6) and improve overall balance compared with artificially fast exoskeleton torque.

To inform the development of balance-improving exoskeletons, we sought to determine whether artificially fast or physiologically delayed ankle ExoBoot (Dephy Inc., Maynard, MA, USA) torque better improves user standing balance compared with a "baseline" condition of no added ExoBoot torque. Because artificially fast torque production may yield suboptimal physiological responses after a disturbance, we hypothesized that delivering delayed balance-correcting ankle ExoBoot torque along with the body's initial reactive ankle moments would better improve user balance compared with baseline. To test this hypothesis, we quantified the standing balance threshold of 10 participants during backward, position-controlled support surface translations with three ExoBoot conditions (movie S1): baseline, artificially fast, and physiologically delayed torque. We defined standing balance threshold as the support surface translation magnitude that causes participants to lose standing balance 50% of the time (28). Throughout each support surface translation, we assessed participant neuromechanics via CoM kinematics, ankle joint and soleus fascicle mechanics, and the initial soleus and tibialis anterior muscle activity (Fig. 1).

RESULTS

Experimental protocol

The evoked support surface translations challenged users' balance by rapidly moving their feet (base of support) posteriorly. The magnitude of each support surface translation was set by an iterative algorithm (29) that estimated participant standing balance threshold at the respective trial's ExoBoot condition. Across trials, ExoBoots randomly produced one of the following torque conditions (Fig. 1): baseline, artificially fast, and physiologically delayed. The baseline ExoBoot condition maintained 1 Nm of plantarflexion torque throughout the trial. The artificially fast ExoBoot condition provided plantar flexor torque beginning 68 ± 11 ms (average ± SD) after perturbation onset, rising to 30 Nm over 50 ms and then declining to 0 Nm over the subsequent 150 ms. The physiologically delayed ExoBoot condition provided plantar flexor torque beginning 171 ± 15 ms after perturbation onset and produced an identical torque profile as the artificially fast condition.

Consistent with our study design, the artificially fast and physiologically delayed ExoBoot conditions provided plantar flexor torque before and along with (or slightly after) the participant's initial reactive joint moments, respectively. During baseline, the participant's largest plantar flexor muscle, the soleus, began producing reactive muscle activity 101 ± 14 ms (average ± SD) after perturbation onset. In turn, B-mode ultrasonography revealed that participant soleus fascicles began shortening 108 ± 22 ms after perturbation onset (8). Because of the delay between initial muscle fascicle shortening and measurable ankle moment production, balance-correcting plantar flexion moments likely initiated about 130 ms after perturbation onset (4, 5).

Standing balance threshold

Artificially fast ExoBoot torque improved participant standing balance threshold compared with baseline, whereas physiologically delayed ExoBoot torque did not. Numerically, participants withstood 9% greater perturbations when the ExoBoots provided an
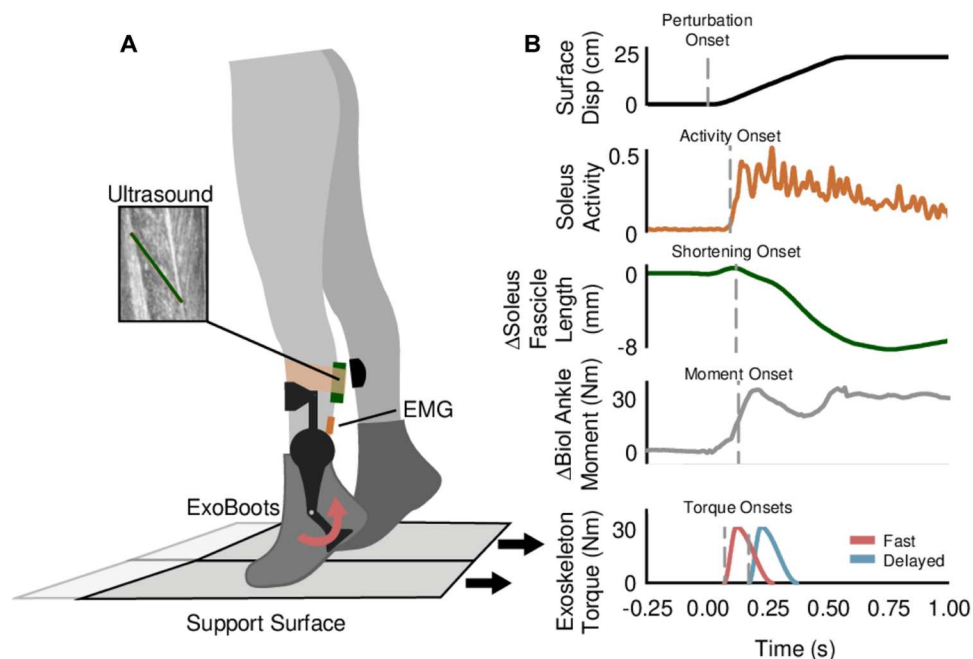

Fig. 1. Balance perturbations and neuromechanical measures. (**A**) Depiction of a backward support surface translation with artificially fast ExoBoot torque (red), a surface EMG electrode (orange), and a B-mode ultrasound probe (green). (**B**) Top to bottom: Theoretical support surface displacement, corresponding processed soleus muscle activity, change in soleus fascicle length, change in biological ankle moment (gray), and the artificially fast (red) and physiologically delayed (blue) exoskeleton torque splines. Vertical dashed lines represent the onset of the indicated parameter(s).

artificially fast torque compared with baseline ($P < 0.001$) (Fig. 2B). However, providing ankle torque along with the body's initial reactive moments did not improve standing balance threshold versus baseline ($P = 0.128$) (Fig. 2B). Together, these data suggest that exoskeletons need to react faster than physiologically capable to improve user standing balance.

Below, we report P values and effect sizes (β) from linear mixed models that describe how ExoBoot torque onset timing influenced salient whole-body, ankle, and underlying agonist and antagonist muscle neuromechanics at a single perturbation magnitude: the participant-averaged baseline standing balance threshold (23.3 cm).

CoM mechanics

Artificially fast ExoBoot torque better kept the user's CoM within the base of support compared with baseline. To reveal how artificially fast ExoBoot torque altered user inverted pendulum mechanics before physiologically delayed torque onset, we assessed CoM kinematics 150 ms after perturbation onset. At 150 ms after perturbation onset, artificially fast ExoBoot torque translated user center of pressure 88% farther forward ($\beta = 3.5$ cm, $P < 0.001$) than baseline. Throughout the support surface translation, this early translation of the center of pressure slightly decreased peak CoM acceleration (ExoBoot and surface displacement interaction, $\beta = -49$ cm/s^2, $P < 0.001$), reduced peak CoM velocity by 17% ($\beta = -10.5$ cm/s, $P < 0.001$), and reduced peak CoM horizontal distance from the base of support by 21% ($\beta = -1.1$ cm, $P = 0.010$) versus baseline (Fig. 3).

Unlike artificially fast torque, physiologically delayed torque onset occurred too late to alter user biomechanics within 150 ms after perturbat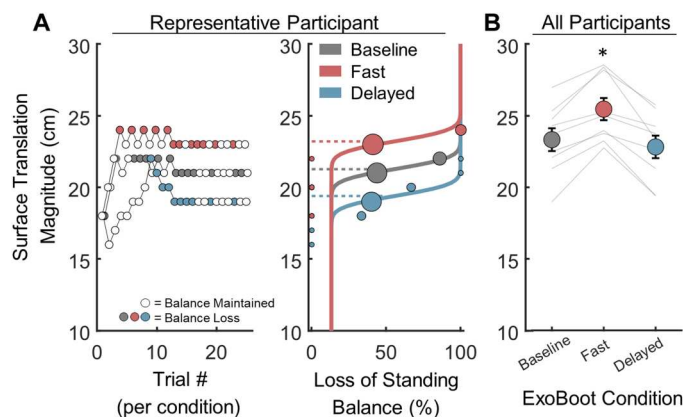ion onset. However, physiologically delayed torque increased the forward translation of the center of pressure by 7% at 300 ms after perturbation onset ($\beta = 0.9$ cm, $P < 0.001$) (Fig. 3A), which slightly reduced peak CoM acceleration ($\beta = -2$ cm/s^2, $P = 0.013$) versus baseline (Fig. 3B). This minor change in CoM acceleration did not measurably reduce peak CoM velocity ($P = 0.143$) or the horizontal displacement from the base of support ($P = 0.471$) with respect to baseline (Fig. 3, C and D).

Ankle mechanics

At the ankle, both artificially fast and physiologically delayed torque increased total joint moments and reduced the dorsiflexion caused by the support surface translation. Artificially fast torque increased total ankle moments during the initial 150 ms after perturbation onset (peak total ankle moment 0 to 150 ms after perturbation onset: $\beta = 10$ Nm, $P < 0.001$) (Fig. 4, A and B). Such moments reduced peak dorsiflexion by 85% ($\beta = -3.9°$, $P = 0.039$) and transitioned the ankle to plantarflexion rotations 57% sooner ($\beta = -110$ ms, $P < 0.001$) than during baseline (Fig. 4, C and D). Within 300 ms of perturbation onset, physiologically delayed torque increased peak total ankle moments 17% ($\beta = 8$ Nm, $P < 0.001$) despite incurring 30% lower biological ankle moments ($\beta = -14$ Nm, $P < 0.001$) versus baseline. These increased total ankle moments reduced peak ankle dorsiflexion by 14% ($\beta = -0.7°$, $P = 0.008$) and initiated plantarflexion 22% earlier compared with baseline ($\beta = -43$ ms, $P = 0.003$) (Fig. 4, C and D).

Muscle fascicle mechanics

By altering ankle mechanics, artificially fast torque virtually eliminated the underlying soleus fascicle tensile force and stretch due to the support surface translation. Specifically, artificially fast torque reduced soleus fascicle force from 70 to 150 ms after perturbation onset (73% less fascicle force at 150 ms after perturbation onset: $\beta = -283$ N, $P < 0.001$) (Fig. 5A). Furthermore, the decreased forces along the muscle-tendon contributed to 76% less peak soleus fascicle stretch ($\beta = -0.3$ mm, $P < 0.001$) and 46% slower peak lengthening velocities ($\beta = 1.8$ mm/s, $P < 0.001$) imposed by the support surface translation (Fig. 5B). Alternatively, physiologically delayed torque did not alter ankle mechanics enough to elicit measurable differences in peak soleus fascicle stretch, velocity, or the time thereof versus baseline (both $P \geq 0.597$) (Fig. 5, A and B).

Reactive muscle activity

Because artificially fast ExoBoot torque reduced CoM excursion (Fig. 3D), ankle dorsiflexion (Fig. 4C), and soleus muscle fascicle force and stretch (Fig. 5, A and B) during the initial 150 ms after perturbation onset versus baseline, the sensory signals driving initial motor responses were likely diminished. Our results demonstrate that artificially fast torque reduced the soleus' initial reactive muscle activity by 18% ($\beta = -0.08$, $P = 0.004$) compared with baseline (Fig. 5C). Neither artificially fast nor physiologically delayed torque altered the latency of the soleus' initial reactive muscle activity ($P \geq 0.284$) versus baseline. Physiologically delayed torque did not affect the amplitude of the soleus' initial reactive muscle activity ($P = 0.079$) versus baseline (Fig. 5). Moreover, in contrast to previous exoskeleton experiments (22–24), the initial reactive muscle activity in the primary antagonist muscle (the tibialis anterior) was unaltered by either experimental ExoBoot condition ($P \geq 0.054$) versus baseline (Fig. 5D).

Fig. 2. Standing balance performance. (**A**) Left: Representative participant's experimental trial order per ExoBoot condition: baseline (gray), artificially fast (red), and physiologically delayed (blue). ExoBoot conditions are randomly interleaved. Filled symbols indicate that the participant was unable to maintain standing balance during the respective trial. Right: The percentage that the representative participant was unable to maintain standing balance at each surface translation magnitude and ExoBoot condition. Symbol size is proportional to the number of experimental trials at the indicated support surface translation magnitude and ExoBoot condition. Solid lines are the psychometric curve fit that we used to determine standing balance threshold, which is the surface translation magnitude where participants were unable to maintain standing balance half of the time. (**B**) Average ± SE standing balance thresholds across ExoBoot conditions (colored symbols) with individual participant data (gray, $n = 9$). Asterisk (*) denotes significance between the artificially fast and the alternative conditions ($P < 0.05$).
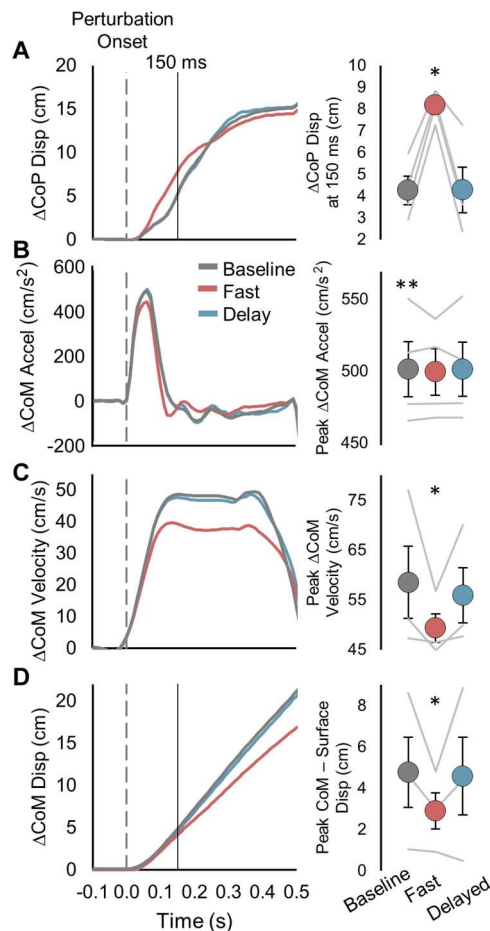
Fig. 3. CoM kinematics. Left: Time series data of average horizontal (A) center of pressure (CoP) displacement, (B) CoM acceleration, (C) CoM velocity, and (D) CoM minus base of support displacement at the same perturbation magnitude. Vertical dashed and solid lines indicate perturbation onset and 150 ms thereafter, respectively. Right: Average ± SE (A) CoP displacement 150 ms after perturbation onset, (B) peak CoM acceleration, (C) peak CoM velocity, and (D) peak CoM minus base of support horizontal displacement, with individual participant data (gray). (A) and (B) contain $n = 4$, and (B) and (C) contain $n = 3$. We only displayed participants who performed successful, balance-maintained trials in each ExoBoot condition at the same perturbation magnitude. Positive y-axis values indicate body movement with respect to the base of support in the direction that the participant is facing. Statistics pertain to all analyzed participants across multiple perturbation magnitudes ($n = 9$). Single asterisk (*) denotes significance between baseline and artificially fast ExoBoot conditions ($P < 0.05$). Double asterisks (**) denote significant interaction between ExoBoot condition and support surface displacement that yields greater peak CoM acceleration in baseline versus the other two conditions ($P < 0.05$).

Further analyses suggest that the initial reactive plantar flexor muscle activity relates better to whole-body mechanics than local ankle or muscle fascicle mechanical changes. Muscle proprioceptors primarily drive the initial burst of reactive muscle activity (*17*, *18*). Accordingly, we compared CoM-, ankle-, and muscle-level parameters that may be encoded by leg muscle spindles and Golgi tendons: CoM acceleration and velocity; biological ankle angle and moment; and soleus fascicle force, length, and velocity. User CoM velocity accounted for 0.27 to 0.45 more variance (0 to
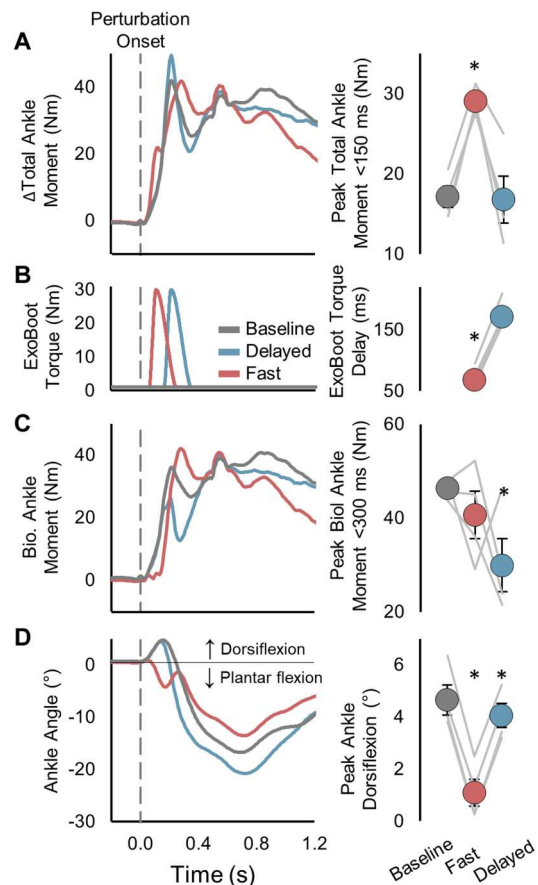

Fig. 4. Ankle mechanics. Left: Time series data of average (A) net ankle moment, (B) ExoBoot torque, (C) net biological (Biol) ankle moments, and (D) ankle angle. Right: Average ± SE (A) peak ankle moment within 150 ms after perturbation magnitude, (B) delay between perturbation onset and ExoBoot torque onset, (C) peak biological ankle moment production throughout the support surface translation (0 to 500 ms), and (D) peak change in ankle dorsiflexion throughout the support surface translation, with individual participant data (gray). Panels contain $n = 4$, except for (B), which includes $n = 8$. We only displayed participants who performed successful, balance-maintained trials in each ExoBoot condition at the same perturbation magnitude. Statistics pertain to all analyzed participants across multiple perturbation magnitudes ($n = 9$). Asterisks (*) denote significance between the indicated artificially fast or physiologically delayed ExoBoot condition and baseline ($P < 0.05$).

1 scale) in the soleus' initial reactive muscle activity compared with each of the aforementioned CoM-, ankle-, and muscle-level parameters across trials ($P \leq 0.001$) (Fig. 6). Within the artificially fast ExoBoot trials, CoM velocity explained 0.57 to 0.78 more variance in the soleus' initial reactive muscle activity than the alternative variables ($P < 0.001$) (Fig. 6).

DISCUSSION

To help overcome unstable characteristics of the human body, triggering balance-correcting exoskeleton torque using mechanical signals may be more effective than using physiological signals, such as using CoM velocity versus muscle activity. Providing ExoBoot torque before the onset of reactive ankle moments improved user balance, whereas delaying torque production to
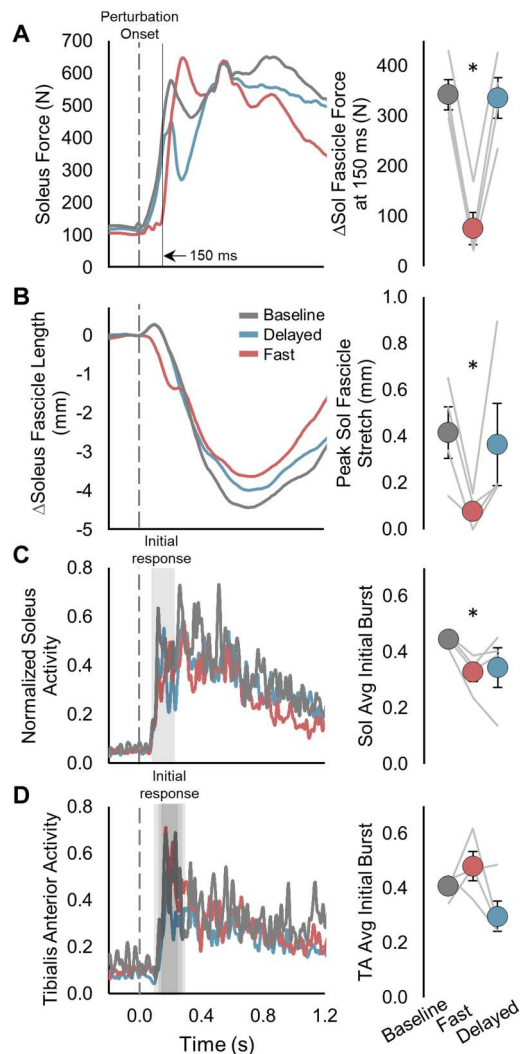
Fig. 5. Soleus neuromechanics. Left: Time series data of average (**A**) soleus fascicle force, (**B**) change in soleus fascicle length, (**C**) normalized soleus activation, and (**D**) normalized tibialis anterior (TA) activation. Vertical dashed and solid lines indicate perturbation onset and 150 ms thereafter, respectively. Shaded regions show the window of the initial burst of reaction muscle activity. Right: Average ± SE (A) soleus fascicle force 150 ms after perturbation onset, (B) peak soleus fascicle stretch, (C) normalized soleus initial reactive muscle activity, and (D) normalized TA initial reactive muscle activity, with individual participant data (gray). Panels contain $n = 4$. We only displayed participants who performed successful, balance-maintained trials in each ExoBoot condition at the same perturbation magnitude. Statistics pertain to all analyzed participants across multiple perturbation magnitudes. Asterisks (*) denote significance between the indicated artificially fast or physiologically delayed ExoBoot condition and baseline ($P < 0.05$).

coincide with the initial physiological reactive ankle moments did not. This finding contrasted with our hypothesis that physiologically delayed torque would improve user balance more than artificially fast torque. Artificially fast torque improved user balance, although it disrupted the initial sensory feedback about the ankles. Despite the disrupted local sensory feedback, the initial reactive ankle muscle activity was fairly consistent across ExoBoot conditions, supporting the notion that initial reactive leg muscle activity is broadly driven by sensory information from throughout the body

and not just the ankle (*5*, *17–19*, *21*). On the basis of these findings, commanding artificially fast balance-correcting exoskeleton torque using global mechanical estimates of sensory feedback, such as CoM kinematics, may predict and precede the user's natural reactive responses to better maintain balance than using local joint- or muscle-level mechanics. Moving forward, these principles of human-exoskeleton balance control may generalize across user neuromechanical states and balance contexts, including walking.

Providing balance-correcting exoskeleton torque faster than physiological reactive joint moments limits the body's initial destabilization after a postural disturbance. The musculoskeletal system's intrinsic mechanical properties set the initial dynamics of a perturbed body (*17*). In particular, leg joints provide a baseline resistance to perturbations (*1*, *2*), which affect body segment accelerations while reactive physiological responses process (*4*, *5*). In our study, artificially fast ExoBoot torque augmented the intrinsic mechanical resistance of the user's body by reducing ankle dorsiflexion and translating the center of pressure forward earlier than baseline. These early mechanical changes improved user balance by decelerating the perturbed CoM and better keeping it within its base of support (*3*). On the contrary, despite producing an identical torque profile, delaying ExoBoot torque to coincide with physiological reaction times did not change the user's mechanics enough to improve user balance. Thus, using an assistive device to "strengthen" participant reactive response may not improve balance as much as implied by previous studies (*30*, *31*).

Artificially fast ExoBoot torque disrupted local ankle mechanics driving sensory encoding, but the ankle's ensuing physiological responses were largely maintained. Unlike that typically observed during backward support surface translations, artificially fast torque essentially prevented the user's ankle joint from dorsiflexing (*19*, *20*, *32*) and, in turn, the underlying soleus fascicles from stretching. Such altered muscle-tendon mechanics practically eliminate initial sensory feedback from agonist ankle muscle spindles and Golgi tendons (*33–38*), the predominant sensory receptors affecting initial reactive muscle activity (*17*, *18*). Alternatively, antagonist leg muscles probably stretched more rapidly because of external tensile forces imposed by artificially fast ExoBoot torque. However, both the ensuing initial reactive agonist (soleus) and antagonist (tibialis anterior) muscle activity hardly changed during the artificially fast condition compared to baseline, indicating that balance-correcting exoskeletons may be able to reposition individual leg joints without concomitant changes in the initial underlying physiological responses.

On the contrary, initial reactive leg muscle activity is thought to be driven by sensorimotor feedback signals throughout the body to accomplish task-level goals (*17–20*), such as maintaining standing balance. Consistent with this theory, across ExoBoot conditions, our participant cohort's reactive soleus activation somewhat resembled perturbed CoM kinematics, which approximate "global" sensorimotor signals (*17*, *19*, *32*). Accordingly, commanding balance-correcting exoskeleton torque using CoM kinematics, or other estimates of global sensory feedback, may act in congruence with subsequent physiological muscle activity. In other words, because CoM kinematics relate to reactive leg muscle activity, tuning exoskeleton torque to the perturbed CoM kinematics should yield symbiotic human-exoskeleton balance responses.

We tested our hypothesis while controlling for the user's neuromechanical state. We regulated participant initial position and
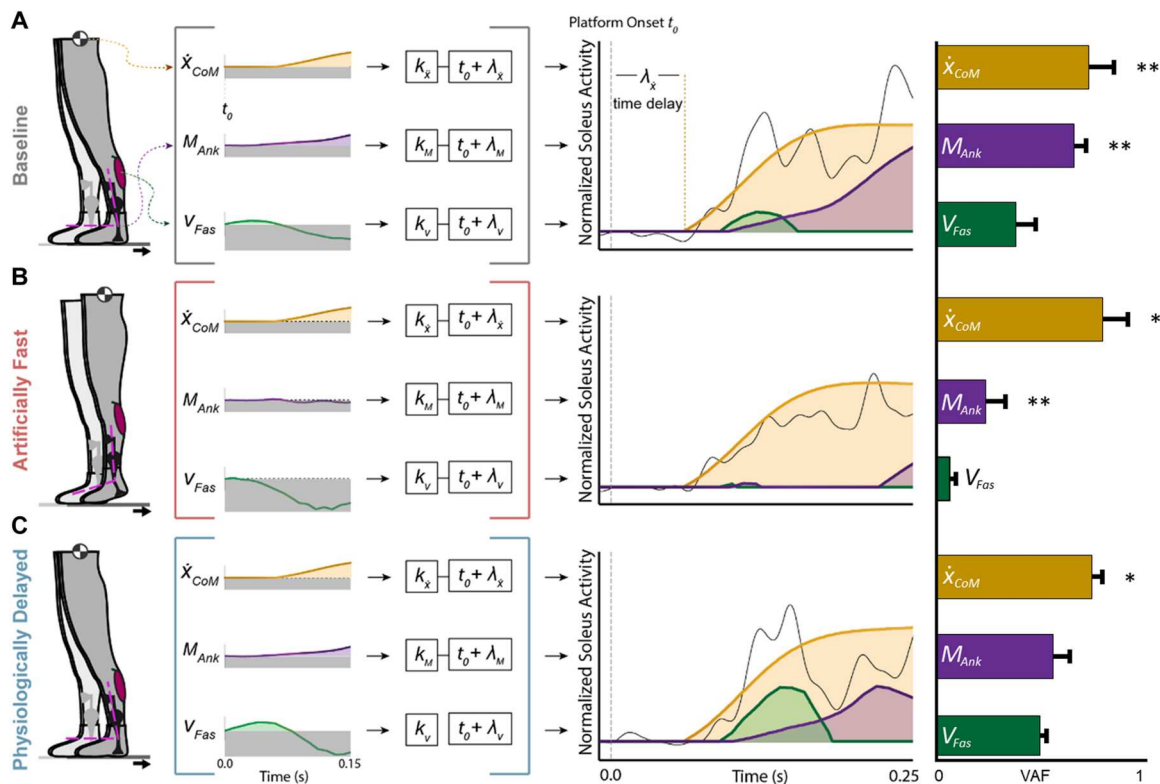
Fig. 6. Global and local mechanics relating to reactive soleus muscle activity. (**Left**) Depiction of support surface translations with each ExoBoot condition about 100 ms after perturbation onset. (**Middle left**) Representative time series of mechanical measures with gains (k_{sub}) and delays (λ_{sub}) added to the time of perturbation onset (t_0) ($n = 1$). (**Middle right**) Representative normalized soleus muscle activity (black line) with the best fit of the corresponding mechanical measures (colored shaded) with tuned gains and a constant delay ($n = 1$). (**Right**) The variance of the soleus' initial reactive muscle activity accounted for (VAF) by each mechanical measure across participants ($n = 8$). (A), (B), and (C) portray baseline, artificially fast, and physiologically delayed ExoBoot conditions, respectively. The three indicated biomechanical measures are CoM velocity (gold, $\dot{x}_{CoM}$), net ankle moment (purple, M_{Ank}), and soleus muscle fascicle lengthening velocity (green, V_{Fas}). Asterisk (*) denotes significance between $\dot{x}_{CoM}$ and other measures ($P < 0.05$). Two asterisks (**) denotes significance between indicated variable and V_{Fas}.

randomized ExoBoot conditions, yielding consistent postural configurations, baseline muscle activity, and feedforward control of the body's intrinsic mechanical properties (*39–41*). Furthermore, the randomization of the ExoBoot conditions controlled for variations in participant central reactive feedback gains (Eq. 3) (*18, 19, 32*), enabling perturbed mechanics to drive user sensorimotor feedback responses. Therefore, we conclude that the observed 18% reduction in reactive soleus muscle activity during the artificially fast versus baseline condition was related to altered sensory feedback, not altered feedforward or feedback control. Despite the scientific merits of our study, people constantly adapt their feedforward and feedback control during daily life (*5, 17*). Thus, to ultimately improve human balance outside of the laboratory, ideal exoskeleton controllers may need to account for the user's constantly changing feedforward and feedback neuromechanical elements.

Our study has potential limitations. We could not identify the exact onset of reactive ankle moments during support surface translations or the precise transfer of device torque to the user. Rather, we estimated the onset of reactive ankle moments using measured soleus muscle activity and literature-estimated delays (10 to 50 ms) (*4, 5, 8*). In addition, we conservatively estimated ExoBoot torque transfer to the user's skeleton using a combination of laboratory signal syncing, computing commanded versus actual device current, approximating human-device interface delays, and

comparing participant inverse dynamics across ExoBoot conditions (see Materials and Methods). Perhaps more precisely aligning device torque to user reactive moments would have enabled physiologically delayed torque to improve user balance compared with baseline. Moreover, we did not directly measure ExoBoot torque. Instead, we relied on motor current, the manufacturer-specified motor constant (*42*), and our characterization of the nonlinear transmission. The evoked motor current was identical between the artificially fast and the physiologically delayed conditions, enabling us to evaluate how ExoBoot torque onset latency influenced standing balance threshold while controlling for device torque amplitude. In addition, there is likely an ideal balance-correcting torque amplitude that depends on device torque onset latency and the body's perturbed dynamics, which affect the user's reactive feedback control (*5*). Accordingly, the ability of artificially fast and physiologically delayed ExoBoot torque to improve user balance can likely be enhanced further than that observed in the present study by tuning device torque amplitude and latency in concert. Human-in-the-loop optimization offers a promising solution for determining ideal exoskeleton torque parameters that enable users to maintain balance during ever-challenging disturbances (*43–46*).

Exoskeletons may need to react faster than physiologically possible to improve user balance across postures and movements. To date, providing exoskeleton torque to user leg joints faster than

physiologically possible has improved user balance during maintained standing (present study) and reactive stepping (11). Consistent with the standing balance results, a previous study showed that providing exoskeleton torque at physiological latencies did not improve user balance during perturbed walking (47). Previous exoskeleton stepping (11, 12) and walking (47) studies used CoM-initiated perturbations, which likely elicited greater initial visual and vestibular sensory feedback than support surface translations (5, 48). However, CoM-initiated perturbations do not yield faster user reactive responses than support surface translations (49, 50). Moreover, across a variety of postural perturbations (18, 19, 32) as well as during walking (51–53), CoM kinematics relate to delayed user reactive balance responses. Hence, placing wearable sensors near the user's CoM may inform balance-correcting exoskeleton torque better than distally located sensors. We envision that exoskeletons for daily use will soon improve user balance by predicting and preceding the underlying physiological responses to postural perturbations.

MATERIALS AND METHODS
Participants
Ten healthy adults participated in this study after providing informed written consent in accordance with the Emory University Institutional Review Board (average ± SD; four female and six male; age, 26.3 ± 2.0 years; height, 1.78 ± 0.12 m; mass, 79.1 ± 13.9 kg).

ExoBoots
After informed consent, participants donned bilateral ExoBoots (EB504; Dephy Inc., USA). Each ExoBoot comprised a commercial boot with a carbon fiber plate embedded in the midsole and a quasi-direct drive actuator mounted laterally that could apply up to 30 Nm of plantarflexion torque. A nonlinear, unidirectional cable-based transmission connected the motor to the ankle joint. Open-loop torque control was implemented via closed-loop current control, with motor torque calculated from current using the manufacturer-specified motor constant [characterized in (42)], and ankle torque was calculated from motor torque using our internal characterization of the nonlinear transmission ratio (generally between 10:1 and 14:1 in the tested range of motion).

A Raspberry Pi 4B read in sensor data and commanded actuator torque at 200 Hz via USB (Raspberry Pi Foundation, UK). Using a custom Python script, we commanded ExoBoots to provide plantarflexion torque after onboard accelerometers detected the onset of a backward support surface translation. The three axes of acceleration signals were high pass–filtered with a second-order, 1-Hz Butterworth filter. A perturbation was detected if ExoBoot acceleration was greater than 147 cm/s^2 in the posterior direction and less than 98 cm/s^2 in both medial and lateral directions in either ExoBoot. During the baseline condition, 1 Nm of plantarflexion was applied to maintain cable engagement. In the artificially fast condition, a piecewise cubic hermite interpolating polynomial with torque is defined as a function of time initiated immediately after perturbation detection (time vector: time = [0 ms, 50 ms, 200 ms] and torque vector: torque = [0 Nm, 30 Nm, 0 Nm]). In the physiologically delayed condition, this same spline was commanded after an additional 100-ms delay (Fig. 1).

We could not identify the precise transfer of ExoBoot torque to the user. Thus, we estimated ExoBoot torque transfer to the user's skeleton using a combination of laboratory sync tests to quantify the delay between (i) perturbation onset and ExoBoot perturbation detection (average ± SD, 14 ± 6 ms), (ii) desired versus measured ExoBoot current (average ± SD, 27 ± 5 ms), as well as by (iii) comparing participant inverse dynamics across ExoBoot conditions (average ± SD; artificially fast: 68 ± 11 ms; physiologically delayed: 171 ± 15 ms). Using inverse dynamics, we assumed that the artificially fast and physiologically delayed trial's initial peak total ankle moment occurred 50 ms after ExoBoot torque onset. From these estimates, artificially fast and physiologically delayed ExoBoot torque initiated between 41 to 68 ms and 141 to 171 ms after perturbation onset, respectively. The range of these estimates indicated that artificially fast and physiologically delayed ExoBoot torque onset occurred earlier and later, respectively, than measured initial reactive soleus muscle activity—enabling us to test our hypothesis. We conservatively interpreted the longest estimate of ExoBoot torque onset throughout the article.

Standing balance threshold
Participants performed standing balance trials on a custom platform with embedded force plates (Factory Automation Systems, USA) (54, 55). Each trial began with participants standing still on a platform, wearing bilateral ExoBoots and a safety harness, with their arms crossed about their torso and each ExoBoot on a separate force plate. In this position, we perturbed participants by commanding the platform to rapidly translate backward (move their feet behind their body) (Fig. 1). We instructed participants to maintain standing balance throughout each trial, which was accomplished if they did not fall (caught by safety harness), take a step, or move their arms from their torso. If participants fell, took a balance-regaining step, or moved their arms from their torso, they were considered unable to maintain standing balance for the respective trial. All backward support surface translations lasted about 500 ms, which we accomplished by scaling platform acceleration and velocity with displacement. After each perturbation, participants stood for at least 4 s before experiencing a subsequent perturbation.

We performed backward support surface translations to determine how each ExoBoot condition affected user standing balance threshold, which is the perturbation magnitude where participants could maintain standing balance in half of the trials. To quantify standing balance threshold for each participant and ExoBoot condition, we conducted 25 perturbations per ExoBoot condition using QUEST, an iterative parameter estimation algorithm (29). QUEST is a Bayesian adaptive psychophysics algorithm that sets each trial to the current best estimated standing balance threshold using a psychometric curve fit from the respective ExoBoot condition's previous trials, including a prior that was set before the experiment (Fig. 2A).

In the QUEST algorithm, some parameters describing the psychometric curve were fixed for the running fit: We used a cumulative normal function as the shape of the psychometric curve, assumed a lapse rate of 3%, fixed the slope at 1, and only allowed threshold to vary (Fig. 2A). During testing, perturbation displacement was rounded to the nearest integer (in centimeters). After all participants completed the experiment, across-participant data were pooled (normalized using previously calculated thresholds)

to calculate across-participant slope and lapse rate values more accurately, which we deemed to be similar for each participant. From these new fixed values (lapse rate, 13%; slope, 1.6), we fit psychometric curves and calculated final standing balance thresholds. We removed standing balance threshold and neuromechanical data from one participant because they preemptively crouched before the support surface translations.

Protocol

Overall, each participant experienced 106 support surface translations. The first six trials were "practice" and involved 12-cm backward support surface translations: two baseline trials, two artificially fast trials, and two physiologically delayed trials. Next, participants experienced 75 backward and 25 forward perturbations. The 75 backward perturbations consisted of 25 trials at each of the three ExoBoot conditions. The 25 forward perturbations were implemented to mitigate the participant's adapting feedforward strategies to consistent backward perturbations (32, 56). We randomized the order of all 100 perturbation trials. To reduce the potential effects of fatigue, participants performed a seated rest for at least 5 min after every 25 trials.

Neuromechanical analyses

To evaluate how artificially fast and physiologically delayed ExoBoot torque influenced user standing balance threshold versus baseline, we analyzed participant neuromechanics (CoM, ankle, and fascicle mechanics as well as muscle activity) during successful balance-maintained trials at two different participant-specific perturbation magnitudes: standing balance threshold for each ExoBoot condition and the highest perturbation magnitude in which there was a successful trial for all three ExoBoot conditions. If there was no perturbation magnitude where the participant successfully maintained standing balance across all three ExoBoot conditions, we analyzed the highest successful perturbation magnitude with two different ExoBoot conditions. Overall, our results were derived from successful experimental trials spanning perturbation magnitudes between 81 and 100% of each participant's standing balance threshold.

CoM and ankle mechanics

We quantified sagittal plane CoM and ankle biomechanics using two-dimensional ground reaction forces (1000 Hz) and a motion capture system that tracked reflective markers over each participant's body (100 Hz). We placed motion capture markers superficial to the body after a custom bilateral Helen Hayes 33-marker set that included the following segments: head-arms-trunk, thigh, shank, and foot. Marker placement was consistent with (19, 57), plus four additional markers per foot ankle (medial malleolus, medial and lateral calcaneus, and head of the fifth metatarsal). We filtered ground reaction forces and marker data using fourth-order low-pass filters with cutoffs of 50 and 10 Hz, respectively. We performed inverse dynamics with the filtered kinematics and force data using OpenSim Gait 2392 model (58). We generated joint angle trajectories by minimizing the tracking error between virtual and experimental marker trajectories: average kinematic marker root mean square error was 1.0 cm, and average maximum marker error was 3.5 cm (59). After inverse dynamics, we calculated the anterior-posterior center of pressure along the foot as well as horizontal CoM acceleration, velocity, and position

throughout each trial using horizontal ground reaction forces and the weighted sum of segment masses (60). Because of motion capture marker disappearance that caused model errors, we omitted inaccurate CoM velocity and position results from four participants (omitted 7 of 27 possible participant-ExoBoot conditions). We computed right ankle angle in addition to total and biological right ankle moment throughout each trial. Total ankle moment was the net ankle moment provided by the exoskeleton torque and biological ankle moment. To calculate biological ankle moment (M_{bio}), we subtracted the commanded exoskeleton torque (τ_{exo}) from the total ankle moment (M_{tot}) (Eq. 1).

$$M_{bio} = M_{tot} - \tau_{exo} \qquad (1)$$

Soleus fascicle mechanics

During each trial, we tracked participant right soleus muscle fascicle lengths and angles using a linear-array B-mode ultrasound probe that was superficial to the medial gastrocnemius (115 Hz; Telemed, Vilnius, Lithuania). We filtered muscle fascicle length and pennation angle using a fourth-order low-pass Butterworth filter (10 Hz). Next, we calculated soleus fascicle force (F_{sol}). To do this, we divided biological ankle moment (M_{bio}) by the Achilles tendon moment arm (r_{AT}) to compute plantar flexor muscle-tendon force. Next, we attributed 46% of the plantar flexor muscle-tendon force to the soleus on the basis of its cross-sectional area relative to all plantar flexor muscles ($CSA_{sol/pf}$) (61). Last, we divided soleus force acting along the muscle-tendon by the cosine of soleus muscle fascicle pennation angle ($\cos\theta_{pen}$), thereby yielding soleus muscle fascicle force (F_{sol}) (Eq. 2).

$$F_{sol} = \frac{\left(\frac{M_{bio}}{r_{AT}}\right)CSA_{sol/pf}}{\cos\theta_{pen}} \qquad (2)$$

Electromyography

During each trial, we recorded surface electromyography (EMG) signals from the participant's right soleus and tibialis anterior muscles (1000 Hz) (Motion Lab Systems Inc., Baton Rouge, LA, USA). We filtered EMG signals using a high-pass third-order zero-lag Butterworth filter (35 Hz). Next, we subtracted the mean value, rectified the signals, and then low pass–filtered the signals. Using the filtered signals, we quantified the duration between perturbation onset and reactive soleus activation, defined as when the EMG signal increased two SDs above the maximum quiet standing value during the 500 ms before perturbation onset for the respective trial. We removed soleus muscle activity data from one outlying participant because they exhibited initial reactive muscle activity that was >5 interquartile ranges beyond the third quartile of the cohort's amplitude. Because of technical issues, we are missing tibialis anterior muscle activity data from one participant's baseline ExoBoot trials.

To find the neuromechanical variable that best relates to the user's initial balance-correcting response, we reconstructed soleus muscle activity during the initial 250 ms after perturbation onset using a sensorimotor response model (17). We ran the model with multiple neuromechanical feedback channels that theoretically relate to sensory feedback: CoM horizontal acceleration and velocity; biological ankle moment and angle; and soleus fascicle force, length, and velocity. For each signal (s), we determined a feedback

gain (k) and time delay (λ) to reconstruct soleus muscle activity (Act$_{rec}$) during the baseline condition (Eq. 3).

$$\text{Act}_{rec} = k_{signal} \cdot s(t - \lambda) \tag{3}$$

Consistent with our study design, we assumed that each participant's initial neuromechanical state was not different across ExoBoot conditions. On the basis of this assumption, we used the same set of gains and delays of each feedback channel to reconstruct the initial soleus activation during the artificially fast and physiologically delayed conditions. To determine the goodness of fit, we calculated the variance of soleus activation that each neuromechanical parameter accounted for.

Statistical analyses

We performed repeated-measures analyses of variance (ANOVAs) to determine whether ExoBoot condition related to standing balance threshold. We performed independent linear mixed models to quantify how ExoBoot condition related to each neuromechanical variable at/over distinct time points: random factor—participants; independent variables—ExoBoot condition and support surface displacement magnitude; dependent variables—center of pressure, CoM acceleration, CoM velocity, CoM excursion, total and biological ankle moment, ankle angle, soleus fascicle force, soleus fascicle velocity, soleus fascicle length, soleus and tibialis anterior initial reactive muscle activity, ExoBoot torque onset latency, and the variance accounted for between soleus initial reactive muscle activity and the aforementioned biomechanical parameters. For every linear mixed model that we performed, we initially ran the model checking for interactions between ExoBoot condition and support surface displacement. If there were no significant interactions, we reran the model with ExoBoot condition and support surface displacement as independent variables. If support surface displacement did not interact with the dependent variable, we dropped support surface displacement from the model and reran it. Otherwise, if there was a significant interaction or effect of support surface displacement, we interpreted the influence of ExoBoot condition on the dependent variable at the baseline standing balance threshold (23.3 cm). We interpreted the effect size of ExoBoot condition on the dependent variable (β). We set significance for all statistical tests as $\alpha = 0.05$ and performed analyses using RStudio (RStudio, Boston, MA, USA).

Supplementary Materials

This PDF file includes:
Data file S1
Movie S1
References

Other Supplementary Material for this manuscript includes the following:
Data file S1
Movie S1

REFERENCES AND NOTES

1. P. G. Morasso, V. Sanguineti, Ankle muscle stiffness alone cannot stabilize balance during quiet standing. *J. Neurophysiol.* **88**, 2157–2162 (2002).
2. I. D. Loram, M. Lakie, Direct measurement of human ankle stiffness during quiet standing: The intrinsic mechanical stiffness is insufficient for stability. *J. Physiol.* **545**, 1041–1053 (2002).
3. D. A. Winter, Human balance and posture control during standing and walking. *Gait Posture* **3**, 193–214 (1995).
4. Y. J. Chang, K. Kulig, The neuromechanical adaptations to Achilles tendinosis. *J. Neurophysiol.* **593**, 3373–3387 (2015).
5. E. R. Kandel, J. H. Schwartz, T. M. Jessell, *Principles of Neural Science* (McGraw Hill, 2000), vol. 4.
6. F. B. Horak, Postural orientation and equilibrium: What do we need to know about neural control of balance to prevent falls? *Age Ageing* **35**, ii7–ii11 (2006).
7. J. Milton, J. L. Cabrera, T. Ohira, S. Tajima, Y. Tonosaki, C. W. Eurick, S. A. Campbell, The time-delayed inverted pendulum: Implications for human balance control. *Chaos* **19**, 026110 (2009).
8. H. L. More, J. M. Donelan, Scaling of sensorimotor delays in terrestrial mammals. *Proc. Biol. Sci.* **285**, 20180613 (2018).
9. A. R. Wu, Human biomechanics perspective on robotics for gait assistance: Challenges and potential solutions. *Proc. Biol. Sci.* **288**, 20211197 (2021).
10. M. F. Hamza, R. A. R. Ghazilla, B. B. Muhammad, H. J. Yap, Balance and stability issues in lower extremity exoskeletons: A systematic review. *Biocybern. Biomed. Eng.* **40**, 1666–1679 (2020).
11. I. Farkhatdinov, J. Ebert, G. van Oort, M. Vlutters, E. van Asseldonk, E. Burdet, Assisting human balance in standing with a robotic exoskeleton. *IEEE Robot. Autom. Lett.* **4**, 414–421 (2019).
12. A. R. Emmens, E. H. Van Asseldonk, H. Van Der Kooij, Effects of a powered ankle-foot orthosis on perturbed standing balance. *J. Neuroeng. Rehabil.* **15**, 50 (2018).
13. T. Zhang, M. Tran, H. Huang, Design and experimental verification of hip exoskeleton with balance capacities for walking assistance. *IEEE ASME Trans. Mechatron.* **23**, 274–285 (2018).
14. V. Monaco, P. Tropea, F. Aprigliano, D. Martelli, A. Parri, M. Cortese, R. Molino-Lova, N. Vitiello, S. Micera, An ecologically-controlled exoskeleton can improve balance recovery after slippage. *Sci. Rep.* **7**, 46721 (2017).
15. R. Pfeifer, M. Lungarella, F. Iida, The challenges ahead for bio-inspired 'soft' robotics. *Commun. ACM* **55**, 76–87 (2012).
16. A. J. Doxon, D. E. Johnson, H. Z. Tan, W. R. Provancher, Human detection and discrimination of tactile repeatability, mechanical backlash, and temporal delay in a combined tactile-kinesthetic haptic display system. *IEEE Trans. Haptics* **6**, 453–463 (2013).
17. L. H. Ting, K. W. van Antwerp, J. E. Scrivens, J. Lucas McKay, T. D. J. Welch, J. T. Bingham, S. P. DeWeerth, Neuromechanical tuning of nonlinear postural control dynamics. *Chaos* **19**, 026111 (2009).
18. D. B. Lockhart, L. H. Ting, Optimal sensorimotor transformations for balance. *Nat. Neurosci.* **10**, 1329–1336 (2007).
19. T. D. Welch, L. H. Ting, A feedback model reproduces muscle activity during human postural responses to support-surface translations. *J. Neurophysiol.* **99**, 1032–1038 (2008).
20. M. G. Carpenter, J. H. Allum, F. Honegger, Directional sensitivity of stretch reflexes and balance corrections for normal subjects in the roll and pitch planes. *Exp. Brain Res.* **129**, 93–113 (1999).
21. M. Vlutters, E. H. van Asseldonk, H. van der Kooij, Ankle muscle responses during perturbed walking with blocked ankle joints. *J. Neurophysiol.* **121**, 1711–1717 (2019).
22. Z. Hasan, Optimized movement trajectories and joint stiffness in unperturbed, inertially loaded movements. *Biol. Cybern.* **53**, 373–382 (1986).
23. R. C. Frysinger, D. Bourbonnais, J. F. Kalaska, A. M. Smith, Cerebellar cortical activity during antagonist cocontraction and reciprocal inhibition of forearm muscles. *J. Neurophysiol.* **51**, 32–49 (1984).
24. M. L. Latash, Muscle coactivation: Definitions, mechanisms, and functions. *J. Neurophysiol.* **120**, 88–104 (2018).
25. A. Nasr, B. Laschowski, J. McPhee, Myoelectric control of robotic leg prostheses and exoskeletons: A review, in *International Design Engineering Technical Conferences and Computers and Information in Engineering Conference* (ASME, 2021), vol. 85444, p. V08AT08A043.
26. A. J. Young, H. Gannon, D. P. Ferris, A biomechanical comparison of proportional electromyography control to biological torque control using a powered hip exoskeleton. *Front. Bioeng. Biotechnol.* **5**, 37 (2017).
27. A. Studnicki, R. J. Downey, D. P. Ferris, Characterizing and removing artifacts using dual-layer EEG during table tennis. *Sensors* **22**, 5867 (2022).
28. J. A. Palmer, A. M. Payne, L. H. Ting, M. R. Borich, Cortical engagement metrics during reactive balance are associated with distinct aspects of balance behavior in older adults. *Front. Aging Neurosci.* **13**, 684743 (2021).
29. A. B. Watson, D. G. Pelli, QUEST: A Bayesian adaptive psychometric method. *Percept. Psychophys.* **33**, 113–120 (1983).
30. M. Jeon, M. O. Gu, J. Yim, Comparison of walking, muscle strength, balance, and fear of falling between repeated fall group, one-time fall group, and nonfall group of the elderly receiving home care service. *Asian Nurs. Res.* **11**, 290–296 (2017).

31. A. C. Alonso, S. M. Ribeiro, N. M. Silva Luna, M. D. Peterson, D. S. Bocalini, M. M. Serra, G. C. Brech, J. M. D'Andrea Greve, L. E. Garcez-Leme, Association between handgrip strength, balance, and knee flexion/extension strength in older adults. *PLOS ONE* **13**, e0198185 (2018).

32. T. D. Welch, L. H. Ting, Mechanisms of motor adaptation in reactive balance control. *PLOS ONE* **9**, e96440 (2014).

33. S. S. Schäfer, S. Kijewski, The dependency of the acceleration response of primary muscle spindle endings on the mechanical properties of the muscle. *Pflugers Arch.* **350**, 101–122 (1974).

34. I. A. Boyd, The response of fast and slow nuclear bag fibres and nuclear chain fibres in isolated cat muscle spindles to fusimotor stimulation, and the effect of intrafusal contraction on the sensory endings. *Q. J. Exp. Physiol. Cogn. Med. Sci.* **61**, 203–253 (1976).

35. V. K. Haftel, E. K. Bichler, T. R. Nichols, M. J. Pinter, T. C. Cope, Movement reduces the dynamic response of muscle spindle afferents and motoneuron synaptic potentials in rat. *J. Neurophysiol.* **91**, 2164–2171 (2004).

36. L. Jami, J. Petit, U. Proske, D. Zytnicki, Responses of tendon organs to unfused contractions of single motor units. *J. Neurophysiol.* **53**, 32–42 (1985).

37. J. Houk, W. Simon, Responses of Golgi tendon organs to forces applied to muscle tendon. *J. Neurophysiol.* **30**, 1466–1481 (1967).

38. B. H. Matthews, Nerve endings in mammalian muscle. *J. Physiol.* **78**, 1–53 (1933).

39. R. Osu, D. W. Franklin, H. Kato, H. Gomi, K. Domen, T. Yoshioka, M. Kawato, Short- and long-term changes in joint co-contraction associated with motor learning as revealed from surface EMG. *J. Neurophysiol.* **88**, 991–1004 (2002).

40. I. G. Amiridis, V. Hatzitaki, F. Arabatzi, Age-induced modifications of static postural control in humans. *Neurosci. Lett.* **350**, 137–140 (2003).

41. J. Jang, K. T. Hsiao, E. T. Hsiao-Weckster, Balance (perceived and actual) and preferred stance width during pregnancy. *Clin. Biomech.* **23**, 468–476 (2008).

42. U. H. Lee, C.-W. Pan, E. J. Rouse, Empirical characterization of a high-performance exterior-rotor type brushless DC motor and drive, in *2019 IEEE/RSJ International Conference on Intelligent Robots and Systems (IROS)* (IEEE, 2019), pp. 8018–8025.

43. P. Slade, M. J. Kochenderfer, S. L. Delp, S. H. Collins, Personalizing exoskeleton assistance while walking in the real world. *Nature* **610**, 277–282 (2022).

44. K. A. Witte, P. Fiers, A. L. Sheets-Singer, S. H. Collins, Improving the energy economy of human running with powered and unpowered ankle exoskeleton assistance. *Sci. Robot.* **5**, eaay9108 (2020).

45. J. Zhang, P. Fiers, K. A. Witte, R. W. Jackson, K. L. Poggensee, C. G. Atkeson, S. H. Collins, Human-in-the-loop optimization of exoskeleton assistance during walking. *Science* **356**, 1280–1284 (2017).

46. Y. Ding, M. Kim, S. Kuindersma, C. J. Walsh, Human-in-the-loop optimization of hip assistance with a soft exosuit during walking. *Sci. Robot.* **3**, eaar5438 (2018).

47. C. Bayón, A. Q. L. Keemink, M. van Mierlo, W. Rampelshammer, H. van der Kooij, E. H. F. van Asseldonk, Cooperative ankle-exoskeleton control can reduce effort to recover balance after unexpected disturbances during walking. *J. Neuroeng. Rehabil.* **19**, 21 (2022).

48. A. M. Payne, G. Hajcak, L. H. Ting, Dissociation of muscle and cortical response scaling to balance perturbation acceleration. *J. Neurophysiol.* **121**, 867–880 (2019).

49. A. Mansfield, B. E. Maki, Are age-related impairments in change-in-support balance reactions dependent on the method of balance perturbation? *J. Biomech.* **42**, 1023–1031 (2009).

50. D. Verniba, W. H. Gage, A comparison of balance-correcting responses induced with platform-translation and shoulder-pull perturbation methods. *J. Biomech.* **112**, 110017 (2020).

51. M. Afschrift, F. De Groote, I. Jonkers, Similar sensorimotor transformations control balance during standing and walking. *PLOS Comput. Biol.* **17**, e1008369 (2021).

52. Y. Wang, M. Srinivasan, Stepping in the direction of the fall: The next foot placement can be predicted from current upper body state in steady-state walking. *Biol. Lett.* **10**, 20140405 (2014).

53. V. Joshi, M. Srinivasan, A controller for walking derived from how humans recover from perturbations. *J. R. Soc. Interface* **16**, 20190027 (2019).

54. S. A. Chvatal, L. H. Ting, Voluntary and reactive recruitment of locomotor muscle synergies during perturbed walking. *J. Neurosci.* **32**, 12237–12250 (2012).

55. S. A. Chvatal, L. H. Ting, Common muscle synergies for balance and walking. *Front. Comput. Neurosci.* **7**, 48 (2013).

56. F. B. Horak, L. M. Nashner, Central programming of postural movements: Adaptation to altered support-surface configurations. *J. Neurophysiol.* **55**, 1369–1381 (1986).

57. G. Martino, J. L. McKay, S. A. Factor, L. H. Ting, Neuromechanical assessment of activated vs. resting leg rigidity using the pendulum test is associated with a fall history in people with parkinson's disease. *Front. Hum. Neurosci.* **14**, 602595 (2020).

58. S. L. Delp, F. C. Anderson, A. S. Arnold, P. Loan, A. Habib, C. T. John, E. Guendelman, D. G. Thelen, OpenSim: Open-source software to create and analyze dynamic simulations of movement. *IEEE Trans. Biomed. Eng.* **54**, 1940–1950 (2007).

59. J. L. Hicks, T. K. Uchida, A. Seth, A. Rajagopal, S. L. Delp, Is my model good enough? Best practices for verification and validation of musculoskeletal models and simulations of movement. *J. Biomech. Eng.* **137**, 020905 (2015).

60. J. L. McKay, K. C. Lang, S. M. Bong, M. E. Hackney, S. A. Factor, L. H. Ting, Abnormal center of mass feedback responses during balance: A potential biomarker of falls in Parkinson's disease. *PLOS ONE* **16**, e0252119 (2021).

61. A. A. Biewener, C. T. Farley, T. J. Roberts, M. Temaner, Muscle mechanical advantage of human walking and running: Implications for energy cost. *J. Appl. Physiol.* **97**, 2266–2274 (2004).

Science Robotics

Exoskeletons need to react faster than physiological responses to improve standing balance

Owen N. Beck, Max K. Shepherd, Rish Rastogi, Giovanni Martino, Lena H. Ting, and Gregory S. Sawicki

View the article online
https://www.science.org/doi/10.1126/scirobotics.adf1080
Permissions
https://www.science.org/help/reprints-and-permissions

Use of this article is subject to the Terms of service